

# How to make graphene superconducting

Gianni Profeta,<sup>1</sup> Matteo Calandra,<sup>2</sup> and Francesco Mauri<sup>2</sup>

<sup>1</sup>*SPIN-CNR - Dipartimento di Fisica Università degli Studi di L'Aquila, I-67100 L'Aquila, Italy*

<sup>2</sup>*IMPMC, Université Paris 6, CNRS, 4 Pl. Jussieu, 75015 Paris, France*

Graphene [1] is the physical realization of many fundamental concepts and phenomena in solid state-physics[2], but in the long list of graphene remarkable properties [3–6], a fundamental block is missing: superconductivity. Making graphene superconducting is relevant as the easy manipulation of this material by nanolytographic techniques paves the way to nanosquids, one-electron superconductor-quantum dot devices[7, 8], superconducting transistors at the nano-scale[9] and cryogenic solid-state coolers[10].

Here we explore the doping of graphene by adatoms coverage. We show that the occurrence of superconductivity depends on the adatom in analogy with graphite intercalated compounds (GICs). However, most surprisingly, and contrary to the GIC case[11, 12], Li covered graphene is superconducting at much higher temperature with respect to Ca covered graphene.

As graphene itself is not superconducting, phonon-mediated superconductivity must be induced by an enhancement of the electron-phonon coupling ( $\lambda$ ),

$$\lambda = \frac{N(0)D^2}{M\omega_{ph}^2} \quad (1)$$

In Eq. 1  $N(0)$  is the electronic density of states (DOS) at the Fermi level,  $D$  is the deformation potential, while  $M$  and  $\omega_{ph}$  are effective atom mass and phonon frequency that in metallic alloys reflect the role of the different atomic species and phonon vibrations involved in superconductivity. In undoped graphene  $\lambda$  is small and phonon-mediated superconductivity does not occur as the small number of carriers, intrinsic in a semimetal, leads to a vanishingly small  $N(0)$ . In this respect the situation is similar to the bulk graphite case, where, without intercalation of foreign atoms superconductivity is not stabilized.

A first guess to induce superconductivity could then be to fill by rigid-band doping the carbon  $\pi$ -states in order to have enough carriers. However, beside the fact that the  $\pi$ -DOS grows very slowly with doping, this hurts against two major difficulties. First, even if the deformation potential related to coupling between  $\pi$ -bands and in-plane phonon vibrations is very large and leads to Kohn anomalies [13], these vibrations are highly energetic ( $\omega_{ph} \approx 0.16$  eV) and  $\lambda$  is suppressed by the  $\omega_{ph}^2$  factor in the denominator. Second, symmetry forbids the coupling between  $\pi$ -states and the softer out-of-planes vibrations.

In order to promote coupling to carbon out-of-plane vibrations it is then necessary to promote new electronic

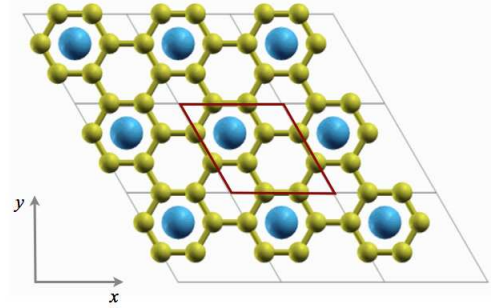


FIG. 1. Crystal Structure of metal adatom covered graphene: yellow (blue) spheres represent carbon (metal) atoms. Adatoms sit on the hollow site of graphene layer.

states at the Fermi level as it happens in GICs. Indeed in superconducting GICs an intercalant bands (interlayer state) occurs at the Fermi level [14] having multiple beneficial effects on  $\lambda$  as (i) the number of carriers is enhanced, (ii) coupling to C out-of-plane vibrations is promoted, (iii) coupling to intercalant vibrations occurs with a corresponding enhancement of the deformation potential and a reduction of the effective  $M\omega_{ph}^2$  term in the denominator of Eq. 1.

In GICs not all kind of intercalant atoms leading to an interlayer state are equally effective in increasing  $T_c$  [15]. The larger  $T_c$  is indeed obtained when the distance ( $h$ ) between the intercalant atom and the graphite plane is smaller. The reason is that the closer the intercalant electrons are to the planes, the larger are the carbon out-of-planes and the intercalant-modes deformation potentials  $D$ . This is demonstrated by the increase of  $T_c$  from  $\text{BaC}_6$  (not superconducting) to  $\text{SrC}_6$  ( $T_c = 1.65$  K)[17] and finally to  $\text{CaC}_6$  ( $T_c = 11.5$  K)[11, 12, 16] and by the increase of  $\text{CaC}_6$  critical temperature under hydrostatic pressure[18].

However a too small intercalant-graphite layer distance could also be detrimental for superconductivity. Indeed the quantum-confinement of the interlayer state in a too narrow region between the planes could result in a up-shift of the intercalant band well above the Fermi energy. In this case the ionization of the intercalant atom is complete and superconductivity is totally suppressed, as in bulk  $\text{LiC}_6$ [14].

Following these accepted guidelines for graphite intercalated compounds, we explore the doping of graphene by foreign-atoms coverage (see Fig. 1) and the possibility in generating superconductivity in graphene by first-

TABLE I. Calculated physical parameters: Optimized structural parameters (in Å), electron-phonon coupling ( $\lambda$ ), logarithmic frequency average ( $\omega_{log}$  in  $\text{cm}^{-1}$ ) and superconducting critical temperature ( $T_c$  in Kelvin) for  $\text{CaC}_6$  and  $\text{LiC}_6$  systems.

	$a$	$h$	$\lambda$	$\omega_{log}$	$T_c$
$\text{CaC}_6$ bulk	4.30	2.19	0.68	284.3	11.5
$\text{CaC}_6$ mono	4.26	2.24	0.40	309.9	1.4
$\text{LiC}_6$ bulk	4.29	1.83	0.33	715.7	0.9
$\text{LiC}_6$ mono	4.26	1.83	0.61	277.8	8.1

principles density functional theory calculations[19, 20].

The parallel with GICs is tempting, and in particular, considering that Calcium intercalated graphite shows the highest superconducting critical temperature among GICs, the first example we consider is Calcium doped graphene and for comparison we simulated Ca intercalated graphite. Calcium, as other alkaline metals, adsorbs in the hollow site of graphene (see Fig.1, TableI)

The electronic band structure of both compounds is reported in Fig. 2 and shows that the deposition of Ca on-top of graphene still preserve the interlayer band at the Fermi level present in the bulk, fundamental for the appearance of superconducting phase in GICs. The removal of quantum confinement along the  $c$ -direction, due to the periodically stacked graphene layers, in passing from the bulk to the monolayer system, lowers the energy of the IL state, that will result more occupied and carbon  $\pi$ -bands less doped.

However, the sole presence of the IL state at the Fermi level being a necessary condition, is not sufficient to guarantee large electron-phonon coupling, unless this state is not coupled with out-of-plane vibrations of graphene lattice. As the localization of the IL state as close as possible to the graphene layer[14, 21, 22] enhances the coupling, in Fig.3 we compare the planar-average of the IL charge density (calculated at the  $\Gamma$ -point of the Brillouin Zone) in the case of bulk and monolayer  $\text{CaC}_6$ .

In the monolayer, the IL charge density spills-out in the vacuum region while in the bulk case, it is much more confined in between the graphene and adatom layers (roughly the region from  $z=0$  Å to  $z=2$  Å).

Based on this last consideration, we can infer that the superconducting critical temperature of  $\text{CaC}_6$  monolayer should be lower than its bulk counterpart. In order to verify this hypothesis, we calculated the vibrational spectrum and the electron-phonon coupling  $\lambda = 2 \int d\omega \alpha^2 F(\omega)/\omega$  of both compounds. The results are summarized in Table I, Fig.4 and Fig.5.

First of all we notice that the monolayer system is dynamically stable, not showing the tendency to displacive instabilities, with a phonon dispersion characterized by three regions: the low energy region of adatom related modes (up to  $300 \text{ cm}^{-1}$ ) extending up to  $400 \text{ cm}^{-1}$  when

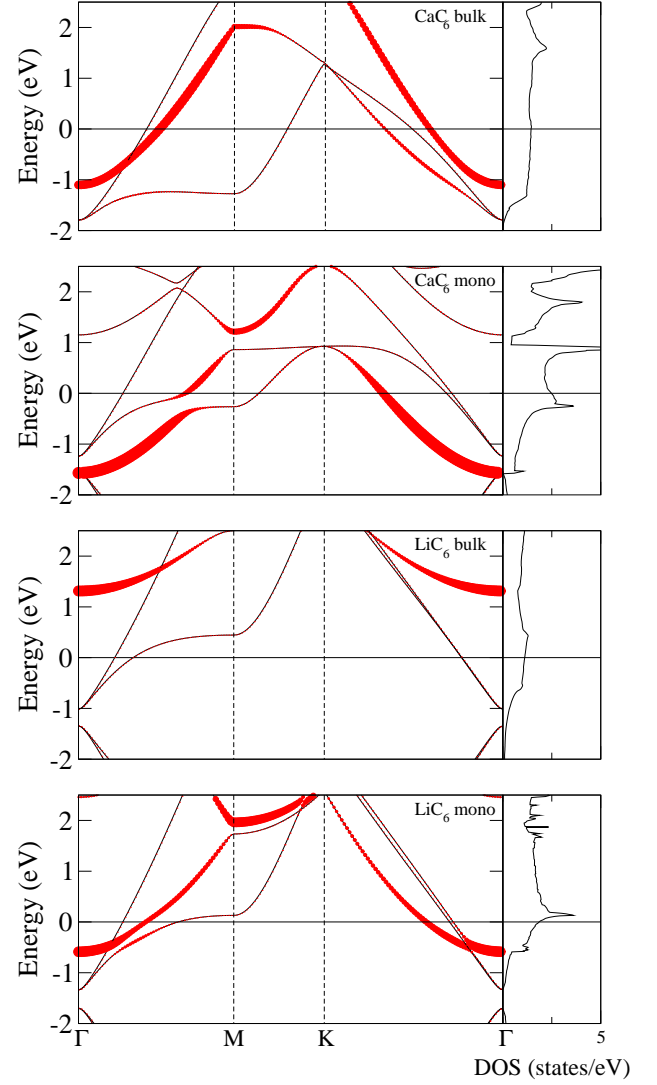


FIG. 2. Electronic band structure: From top to bottom: band structure of  $\text{CaC}_6$  bulk compound (plotted along the high symmetry lines of the monolayer lattice),  $\text{CaC}_6$  monolayer and  $\text{LiC}_6$  bulk and monolayer. Thickness of the bands is proportional to the intercalate/adatom  $s$  character. The Fermi energy is set at zero.

mixed with carbon out-of-plane modes ( $C_z$ ), an intermediate region of  $C_z$  modes ( $400\text{-}900 \text{ cm}^{-1}$ ) and the high energy region characterized by C-C stretching modes.

The major difference between bulk and monolayer cases is the softening of Ca vibrations. From the inspection of the  $\alpha^2 F(\omega)$  (which gives the contribution of each frequency to the total electron-phonon coupling), we note the low contribution of the  $C_z$  modes (around  $500 \text{ cm}^{-1}$ ) to the total electron-phonon coupling in the monolayer case with respect to the bulk  $\text{CaC}_6$ , as expected from the above considerations. While the critical temperature of the bulk compound is 11.5 K (see Methods) in the monolayer case it lowers down to 1.4 K.

This scenario suggests that, as a general rule, the re-

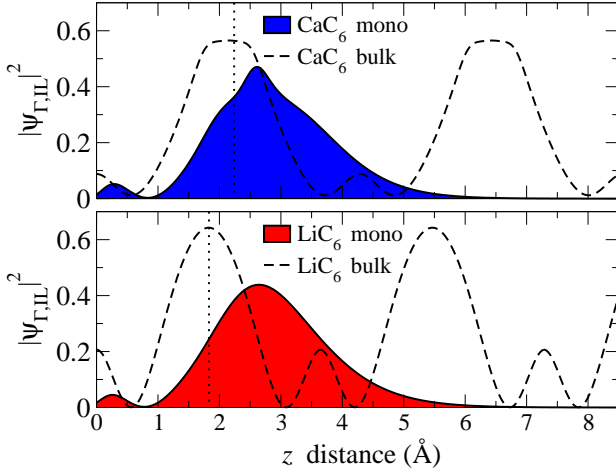


FIG. 3. Interlayer state wavefunction: Planar (in the  $xy$  direction) average of  $|\phi_{\Gamma,IL}|^2$  along the perpendicular (with respect to the graphene layer) direction ( $z$ ). Vertical dashed lines represent  $z$ -position of Ca and Li adatoms.

moval of quantum confinement should be detrimental for the electron-phonon coupling when compared with respect to same bulk (three dimensional periodic) system, due to the shift of the IL wavefunction away from the graphene layer. Every metal covered graphene should have (at least in the same stoichiometry) a reduced superconducting critical temperature with respect to the corresponding GIC.

However, there is at least one case (to the best of our knowledge) among GICs that can be further explored, namely stage-1 Lithium intercalated compound,  $\text{LiC}_6$ [23], in which the IL state is completely empty (see Fig. 2), as the strong confinement along the  $z$  direction (Fig.3) prevents its occupation and for this reason it is not superconducting. In this case, removal of confinement along  $c$  direction (Fig.3) should bring the IL at the Fermi level, as confirmed by the calculated band structure (Fig.2). Inspection of Fig.3 shows that the spatial extension of the IL for Li is the same as in Calcium, but being the IL strongly localized around the adatom and due its closer position to the graphene layer, we can expect an enhancing of the total electron-phonon coupling.

The phonon spectrum confirms, even in this case, the dynamical stability of the monolayer system and the comparison with the bulk counterpart reveals that low energy adatom modes and carbon vibrations in the direction perpendicular to the plane are strongly softened in the monolayer. This suggests that the first two phonon branches, related to the in-plane displacements of Li atoms, and the undispersing Einstein mode displacing Li and C atoms out-of-phase along the  $z$ -direction at around  $500 \text{ cm}^{-1}$ , should undergo enhanced electron-phonon coupling with respect to the bulk. On the contrary, in the  $\text{CaC}_6$  monolayer, adatom vibration and C vibrations along  $z$  are essentially at the same energy as

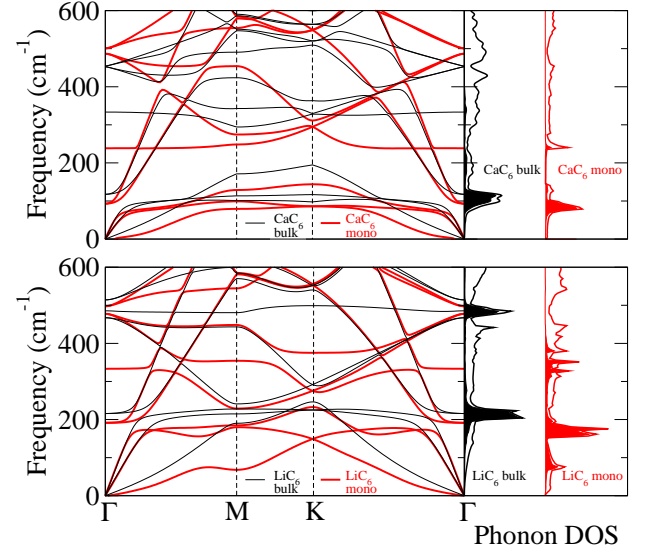


FIG. 4. Dynamical properties: Phonon frequencies dispersion and phonon density of states (PDOS) of  $\text{CaC}_6$  (upper panel) and  $\text{LiC}_6$  (lower panel). Bulk (black) and monolayer (red) cases are considered resolving the adatom (shaded) contribution to the total (solid line) PDOS.

in bulk  $\text{CaC}_6$ .

We found that bulk  $\text{LiC}_6$  is a weak electron-phonon coupling  $\lambda = 0.33$  superconductor with an estimated superconducting critical temperature  $T_c = 0.9\text{K}$ [24], theoretically confirming the absence of superconductivity in  $\text{LiC}_6$ . In the case of monolayer  $\text{LiC}_6$ , the total electron-phonon coupling is  $\lambda = 0.61$ , with a relevant enhancement of the superconducting critical temperature up to  $8.1 \text{ K}$ . The main contributions to the electron-phonon coupling come from the low-energy Li modes and carbon vibrations along  $z$ , as expected from the above considerations, with a appreciable contribution from C-C stretching modes (0.1).

In summary, the ideal conditions for inducing superconductivity in graphene are (i) bring the interlayer state at the Fermi energy (ii), localize it as close as possible to the graphene plane. This will ensure that the presence of the interlayer state effectively switch-on the dormant electron-phonon coupling of  $C_z$  modes that are inactive in the bulk. In addition, the in-plane displacement of adatoms will promote two additional scattering mechanisms, an intra-band contribution due to the interlayer state and an inter-band one due to the interlayer- $\pi$  scattering. *Graphene can be made superconducting by the deposition of Li atoms on the top of it.*

As Li readily intercalates into graphite even at  $100 \text{ K}$ [25] it is possible to incorporate Li atoms even below the graphene sheet. This possibility, based on our calculations, is indeed favorable with respect to the developing of a superconducting phase. In fact, the double adsorption should double the presence of the interlayer state at

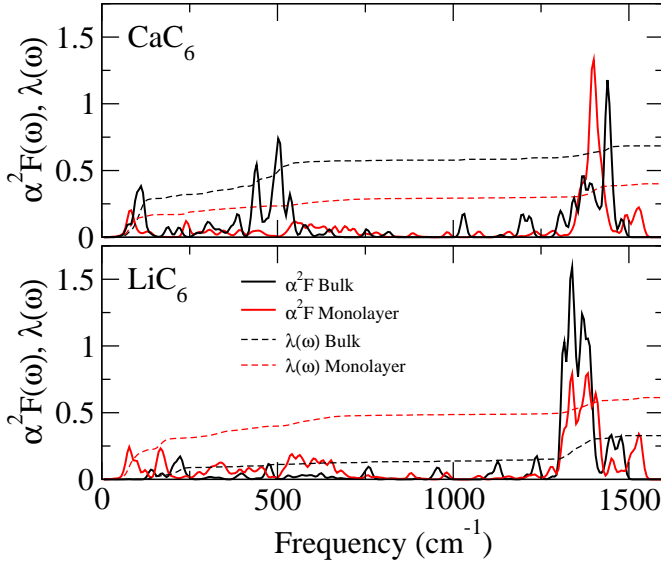


FIG. 5. Eliashberg function:  $\text{CaC}_6$  and  $\text{LiC}_6$  (bulk and monolayer)  $\alpha^2 F(\omega)$ . In the same graph is reported  $\lambda(\omega)$ .

the Fermi level (one coming from each side of graphene) as we indeed verified.

$\text{Li}_2\text{C}_6$  shows an increased coupling in all the frequency range due to the additional strongly coupled interlayer bands, with an electron-phonon coupling of 1.0 giving rise to critical temperature around 17-18 K.

We conclude noting once more that bulk  $\text{LiC}_6$  undergoes a remarkable metal-to-superconductor transition when exfoliated to one layer. The reason is that in a single layer  $\text{LiC}_6$  the interlayer state cross the Fermi level, enhances the electron-phonon coupling and induces superconductivity. Our work demonstrates that superconducting properties of adatoms on graphene are very different from their bulk GIC counterparts.

## METHODS

The results reported in the present paper were obtained from first-principles density functional theory in the local density approximation[20]. The QUANTUM-ESPRESSO[19] package was used with norm-conserving pseudopotentials and a plane-wave cut-off energy of 65 Ry. All the structures considered were relaxed to their minimum energy configuration following the internal forces on atoms and the stress tensor of the unit cell.

The monolayer systems were simulated in the  $\sqrt{3} \times \sqrt{3} R30^\circ$  in-plane unit cell (with respect to standard graphene lattice, see Fig.1) with one adatom per unit cell. Phonons frequencies were calculated in the linear-response technique on a phonon wavevector mesh of  $12 \times 12$  with a  $14 \times 14$  uniform electron momentum grid. The electron-phonon coupling parameter was calculated with electron momentum  $k$ -mesh up to  $40 \times 40$ .

$\text{CaC}_6$  bulk compound was simulated in the experimentally found structure with  $\alpha\beta\gamma$  stacking[11] with a uniform electron-momentum  $k$ -mesh integration of  $8 \times 8 \times 8$ . The phonon frequencies were calculated on a  $4 \times 4 \times 4$  phonon-momentum mesh and the electron-phonon coupling integrated on a  $20 \times 20 \times 20$  electron-momentum mesh.

Bulk  $\text{LiC}_6$  has an  $\alpha\alpha$  stacking and was simulated with and electron-momentum mesh of  $12 \times 12 \times 10$  and  $6 \times 6 \times 6$  phonon-momentum grid for the calculation of phonon frequencies. A  $30 \times 30 \times 25$  electron-momentum mesh was used for the electron-phonon coupling.

The Eliashberg function  $\alpha^2 F(\omega)$  is defined as:

$$\alpha^2 F(\omega) = \frac{1}{N(0)N_k} \sum_{\mathbf{k}, \mathbf{q}, \mathbf{m}, \nu} |g_{\mathbf{k}\mathbf{n}, \mathbf{k}+\mathbf{q}\mathbf{m}}^\nu|^2 \times \delta(\varepsilon_{\mathbf{k}\mathbf{n}}) \delta(\varepsilon_{\mathbf{k}+\mathbf{q}\mathbf{m}}) \delta(\omega - \omega_{\mathbf{q}}^\nu) \quad (2)$$

The total electron-phonon coupling  $\lambda(\omega)$  plotted in Fig.5 is defined as:

$$\lambda(\omega) = 2 \int_0^\omega d\omega' \frac{\alpha^2 F(\omega')}{\omega'} \quad (3)$$

The total electron-phonon coupling is  $\lambda(\omega \rightarrow \infty)$ . The superconducting critical temperature was estimated using the Allen-Dynes formula with  $\mu^* = 0.115$ , which fits the experimental critical temperature measured in  $\text{CaC}_6$  GIC[11].

Work supported by: CINECA-HPC ISCRA grant, by the EU DEISA-SUPERMAG project and by a HPC grant at CASPUR. Part of the calculation were performed at the IDRIS supercomputing center (project 91202).

- [1] K. S. Novoselov *et al.*, Electric Field Effect in Atomically Thin Carbon Films, *Science* **306**, 666 (2004).
- [2] A. K. Geim, Graphene: Status and Prospects, *Science* **324**, 1530 (2009).
- [3] M. I. Katsnelson, K. S. Novoselov and A. K. Geim, Chiral tunnelling and the Klein paradox in graphene, *Nature Physics* **2**, 620 (2006).
- [4] K. S. Novoselov *et al.*, Room-Temperature Quantum Hall Effect in Graphene, *Science* **315** 1379 (2007).
- [5] Y. Zhang, Y. W. Tan, H. L. Stormer, P. Kim, Experimental observation of the quantum Hall effect and Berry's phase in graphene, *Nature* **438**, 201 (2005).
- [6] R. R. Nair *et al.*, Fine Structure Constant Defines Visual Transparency of Graphene, *Science*, **320**, 1308 (2008).
- [7] S. De Franceschi, L. Kouwenhoven, Ch. Schöenberger and W. Wernsdorfer, Hybrid superconductor-quantum dot devices, *Nature Nanotechnology* **5**, 703 (2010).
- [8] M. Huefner *et al.*, Scanning gate microscopy measurements on a superconducting single-electron transistor, *Phys. Rev. B* **79**, 134530 (2009).
- [9] J. Delahaye *et al.*, Low-Noise Current Amplifier Based on Mesoscopic Josephson Junction, *Science* **299**, 1045 (2003).
- [10] Olli-Pentti Sara *et al.*, Heat-Transistor: Demonstration of gate-controlled electronic refrigeration, *Phys. Rev. Lett.* **99**, 027203 (2007).
- [11] N. Emery *et al.*, Superconductivity of Bulk  $\text{CaC}_6$ , *Phys. Rev. Lett.* **95**, 087003 (2005).
- [12] T. Weller *et al.*, Superconductivity in the intercalated graphite compounds  $\text{C}_6\text{Yb}$  and  $\text{C}_6\text{Ca}$ , *Nature Phys.* **1**, 39 (2005).
- [13] S. Piscanec *et al.*, Kohn Anomalies and Electron-Phonon Interactions in Graphite, *Phys. Rev. Lett.* **93**, 185503 (2004).
- [14] G. Csányi *et al.*, The role of the interlayer state in the electronic structure of superconducting graphite intercalated compounds, *Nature Physics* **1**, 42 (2005).
- [15] M. Calandra and F. Mauri, Possibility of superconductivity in graphite intercalated with alkaline earths investigated with density functional theory, *Phys. Rev. B* **74**, 094507 (2006).
- [16] The distance from the graphene plane can be correlated with the ionic radii  $r$ . For the alkalis and alkaline-earths considered they are  $r(\text{Li}) = 0.76\text{\AA}$ ,  $r(\text{Ca}) = 1.0\text{\AA}$ ,  $r(\text{Sr}) = 1.18\text{\AA}$ ,  $r(\text{Ba}) = 1.35\text{\AA}$ .
- [17] J. S. Kim *et al.*, Superconductivity in Heavy Alkaline-Earth Intercalated Graphites, *Phys. Rev. Lett.* **99**, 027001 (2007).

- [18] A. Gauzzi *et al.*, Enhancement of Superconductivity and Evidence of Structural Instability in Intercalated Graphite  $\text{CaC}_6$  under High Pressure, *Phys. Rev. Lett.* **98**, 067002 (2007).
- [19] P. Giannozzi *et al.*, QUANTUM ESPRESSO: a modular and open-source software project for quantum simulations of materials, *J. Phys. Condens. Matter* **21**, 395502 (2009).
- [20] J. P. Perdew and A. Zunger, Self-interaction correction to density-functional approximations for many-electron systems, *Phys. Rev. B* **23**, 5048 (1981).
- [21] M. Calandra and F. Mauri, Theoretical Explanation of Superconductivity in  $\text{C}_6\text{Ca}$ , *Phys. Rev. Lett.* **95**, 237002 (2005).
- [22] L. Boeri *et al.*, Electron-phonon interaction in graphite intercalation compounds, *Phys. Rev. B* **76**, 064510 (2007).
- [23] D. Guerarda and A. Herold, Intercalation of lithium into graphite and other carbons, *Carbon* **13**, 337 (1975).
- [24] The estimated critical temperatures for low  $\lambda$  values are affected by an exponentially increasing error. Within the scope of the present paper, calculated  $T_c$  lower than 1K can be considered as 0K.
- [25] M. Caragiu and S. Finberg, Alkali metal adsorption on graphite: a review, *J. Phys.: Condens. Matter* **17** R 995 (2005).